

## **Relationships between dielectric breakdown resistance and charge transport in alumina materials**

M. Touzin (a), D. Goeuriot (a), X. Meyza (a), C. Guerret-Piécourt (b), D. Juve (c), D. Treheux (c), H.-J. Fitting (d)

(a) Centre Sciences des Matériaux et des Structures, UMR-CNRS 5146, Ecole Nationale Supérieure des Mines de Saint-Etienne, 158 cours Fauriel, F-42023 Saint-Etienne cedex 2, France

(b) Laboratoire de Physico-Chimie des polymères, UMR-CNRS 5067, Université de Pau, BP 1157, F-64013 Pau cedex, France

(c) Laboratoire de Tribologie et Dynamique des Systèmes, UMR-CNRS 5513, Ecole Centrale de Lyon, 36 avenue Guy de Collongue, F-69134 Ecully cedex, France

(d) Physics Department, University of Rostock, Universitätsplatz 3, D-18051 Rostock, Germany

**Keywords :** Al<sub>2</sub>O<sub>3</sub>, Dielectric breakdown

### **Abstract**

Dielectric breakdown is the main cause of insulator degradation. Breakdown strength strongly depends on materials microstructure (grain size, grain boundaries nature...)<sup>1</sup>. The experimental study of these materials behaviour towards charges injection was performed by Scanning Electron Microscopy Mirror Effect (SEMME) method. It allows to know, during the injection, the amount of injected charges and those which are trapped in the insulator. In order to explain the experimental results, we have developed an iterative computer simulation of the self-consistent charge transport in bulk alumina samples during electron beam irradiation, based on the H.-J. Fitting's Flight Drift Model (FDM). Ballistic and drift electron and hole transport as well as their recombination, trapping and detrapping (due to the temperature) are taken in account. As a main result the time dependent secondary electron emission rate and the spatial distributions of currents, charges, the field and the potential slope are obtained. The analysis of these two kinds of results allowed us to identify the effect of the microstructure on the behaviour of the injected charges in the insulator and then to propose, depending on the temperature, some mechanisms leading to a good dielectric breakdown resistance. Indeed, at room temperature a huge localisation of charges limits their injection into the sample which permit to delay breakdown. On the other hand, when the temperature increases, the efficiency of the charges spreading behaviour is improved. In this case, the good breakdown resistance depends on the ability of the charges to diffuse in the materials.

## Introduction

The dielectric properties of insulators, and specially dielectric strength, strongly depend on microstructure. Moreover, temperature has a huge influence on charge transport properties and then on the materials dielectric breakdown resistance. Fig. 1 shows the evolution of dielectric strength with temperature for two kinds of alumina materials : one with an highly-crystallized intergranular phase and the other one with a vitreous one<sup>2</sup>.

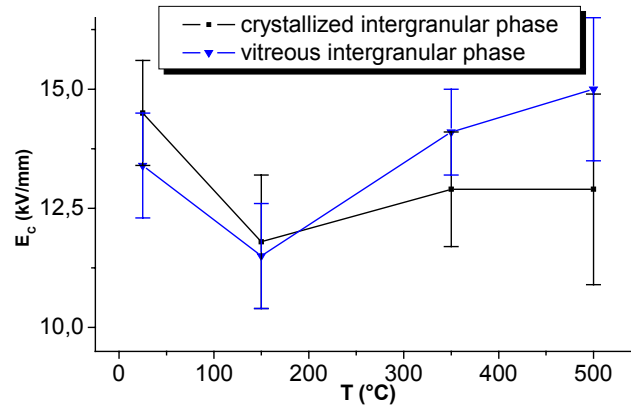


**Figure 1 : Breakdown strength versus temperature for two intergranular phase crystallization states**

First, we observe a decrease of dielectric strength when temperature increases from 20 °C up to 150 °C, then it increases up to 500 °C. We can also notice that at room temperature the best dielectric strength value is linked to the crystallized intergranular phase material but at higher temperature it is the opposite. That proves that microstructure has an influence on charge transport mechanisms. In this work, a correlation is proposed between breakdown events, microstructure parameters and charge transport mechanisms.

## Principle of the simulation

The Flight Drift Model (fig. 2) developed by H.-J. Fitting allowed us to simulate the self-consistent charge transport and charging-up of insulating  $\text{Al}_2\text{O}_3$  samples during electron bombardment. This model is an evolution of the one used by X. Meyza *et al*<sup>3</sup> to calculate the secondary electron emission and self-consistent charge transport and storage in alumina bulk insulators. In this new model, we consider, in addition with the electrons and holes ballistic current, a drift current. Moreover, we take into account the role of the temperature on the charges detrapping by considering the Poole-Frenkel (PF) effect. So, we can write the ballistic current for electrons (E) in reverse and transmission (T) direction :

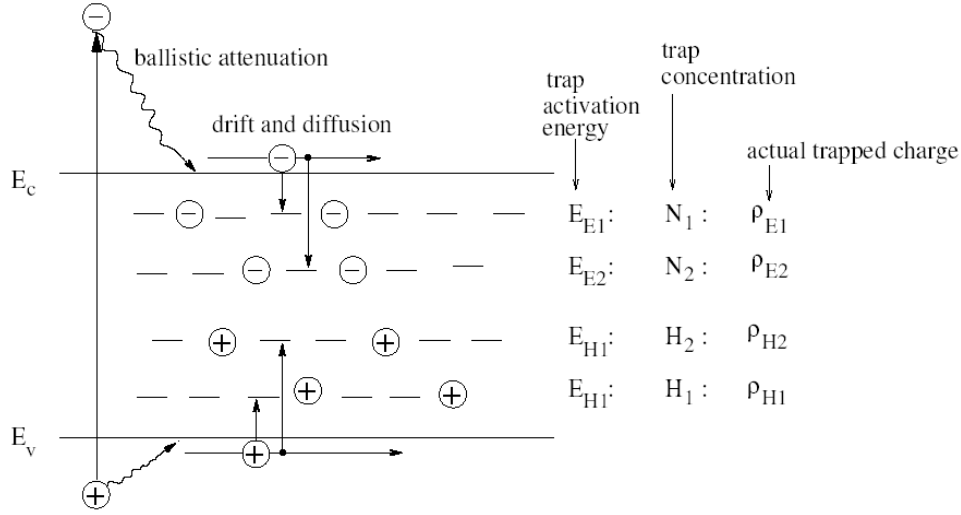


**Figure 2 : Energy band scheme with excited, drifting and trapped electrons and holes.**

So, we can write the ballistic current for electrons (E) in reverse and transmission (T) direction :

$${}_B j_{ET}^{ER}(x) = \left[ \underbrace{{}_B j_{ET}^{ER}(x \pm \Delta x)}_{\text{convection}} + \underbrace{\frac{1}{2} j_0 g_i(x, E'_0) \cdot \Delta x}_{\text{generation}} \right] \underbrace{W_{EF}}_{\text{attenuation}}$$

As well for holes (H) :

$${}_B j_{HT}^{HR}(x) = \left[ \underbrace{{}_B j_{HT}^{HR}(x \pm \Delta x)}_{\text{convection}} + \underbrace{\frac{1}{2} j_0 g_i(x, E'_0) \cdot \Delta x}_{\text{generation}} \right] W_{HF}$$

$g_i$  is the inner secondary electrons generation rate.

$j_0$  is the impinging primary electrons current density.

$E'_0$  is the electron beam energy  $E_0$  modified by the surface potential  $V_0$  :  $E'_0 = E_0 + eV_0$ .

$W_{E/HF}$  is an attenuation probability which depends on the field strength  $F$ .

After the ballistic current attenuation, the charges are responsible of a drift current which can be written :

for electrons (E) :

$${}_D j_{ET}^{ER}(x) = \left[ \underbrace{{}_D j_{ET}^{ER}(x \pm \Delta x)}_{\text{convection}} + \underbrace{{}_B j^{ER}(x + \Delta x)(1 - {}^R W_{EF}) + {}_B j_{ET}(x - \Delta x)(1 - {}^T W_{EF})}_{\text{ballistic flux}} + \underbrace{\rho_{E1}(x) W_{EPF}}_{\text{detrapping (PF)}} \right] \times \underbrace{{}_D F_{ET}^{ER}(x) \cdot W_{EH} \cdot W_{E1} \cdot W_{E2}}_{\text{drift factor}}$$

a : recombination  
 b : shallow trapping  
 c : deep trap capture

and for holes (H) :

$${}_D j_{HT}^{HR}(x) = \left[ \underbrace{{}_D j_{HT}^{HR}(x \pm \Delta x)}_{\text{convection}} + \underbrace{{}_B j^{HR}(x + \Delta x)(1 - {}^R W_{HF}) + {}_B j_{HT}(x - \Delta x)(1 - {}^T W_{HF})}_{\text{ballistic flux}} + \underbrace{\rho_{H1}(x) W_{HPF}}_{\text{detrapping (PF)}} \right] \times \underbrace{{}_D F_{HT}^{HR}(x) \cdot W_{HE} \cdot W_{H1} \cdot W_{H2}}_{\text{drift factor}}$$

The drift factor  $D F$  is an effective current-anisotropy factor weighting the initial currents with and against the electric field.

Trapped charge  $\rho(x)$  can be calculated from the drift currents. The field distribution  $F(x)$  is obtained by introduction of  $\rho(x)$  in the Poisson equation and so the potential slope  $V(x,t)$  by integration of the field strengths.

The program still need optimisation, so some examples will be presented at the conference.

## Results

It is possible to correlate the experimental results obtained by the SEMME method with the numerical simulation. Fig. 3 shows the absorbed current variations for two kinds of alumina materials at two temperatures.

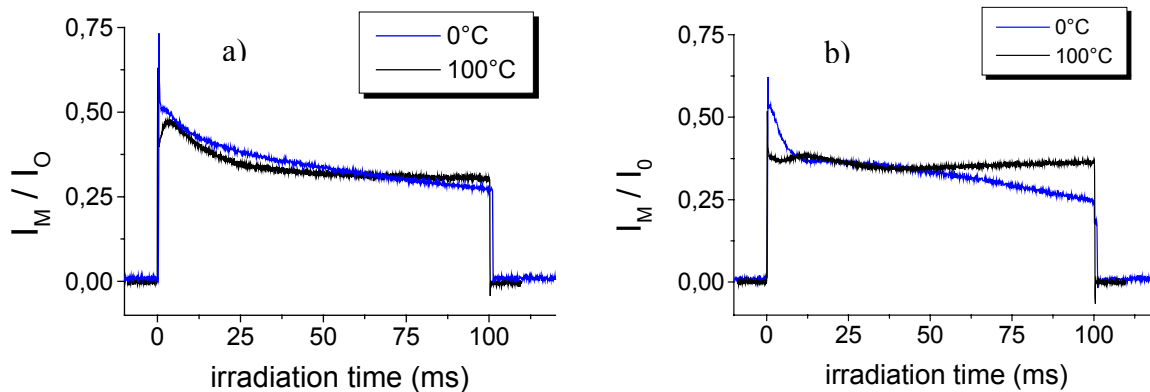


**Figure 3 : Absorbed current variations for two kinds of alumina materials : a) with a crystallized intergranular phase and b) with a vitreous intergranular phase**

The very abrupt decrease we observe at the beginning of the injection at  $0^\circ\text{C}$  for the material with a crystallized secondary phase, can be associated to the huge localization of negative charges near the sample surface investigated via the simulation. This localization causes the apparition of a very negative surface potential which limits the injection of new charges into the sample. In the case of the vitreous secondary phase material, the decrease is less abrupt. That could be attributed to the difference of trapping behaviour between these two materials (there are certainly more traps and deeper in the crystallized phase than in the vitreous one) . At  $100^\circ\text{C}$ , the charges are not stabilized and the simulation shows a charge diffusion behaviour. It is confirmed by the form of the experimental curves : they take a crenel form.

## Conclusion

Correlation between experimental and simulated results allowed us to distinguish two different charge transport behaviours depending on the ability of the material to trap and stabilize charges which is connected to the intergranular phase nature. It appears that at low temperature all charges are trapped and the dielectric breakdown is delayed because of the increase of the internal electric field threshold magnitude. This process is more efficient in the crystallized intergranular phase material. At higher temperature, the detrapping process is activated. It allows a charges spreading behaviour which keeps the internal electric field under the critic value. This phenomenon is promoted by a vitreous intergranular phase. At

intermediate temperature, the dielectric breakdown field decrease can be explained by the transition between the two behaviours. The charges are less trapped but the spreading behaviour is not sufficient enough to keep the charge density low.

---

<sup>1</sup> J. Liebault, J. Vallayer, D. Goeuriot, D. Tréheux, F. Thévenot, “How the trapping of charges can explain the dielectrics breakdown performance of alumina ceramics”, *J. Eur. Ceram. Soc.*, 2001, **21**, pp. 389-397

<sup>2</sup> X. Meyza, “Relations microstructure – comportement face à l’injection de charges – rigidité diélectrique pour des alumines polycristallines, effet de la température et d’un vieillissement thermique », PhD thesis, Ecole Nationale Supérieure des Mines de Saint-Etienne, 2003

<sup>3</sup> X. Meyza, D. Goeuriot, C. Guerret-Piécourt, D. Tréheux, H.-J. Fitting, “Secondary electron emission and self-consistent charge transport and storage in bulk insulators : Application to alumina”, *J. Appl. Phys.*, 2003, **94**, pp. 5384-5392